

## Authors' Response to the Reviewer Comments

**Manuscript title: Critical Role of Dust Induced Electrostatic Coagulation in the Evolution of Aerosol Size Distributions in the Atmosphere**

**Journal: Atmospheric Chemistry and Physics**

**Manuscript ID: egusphere-2026-486**

### Response to Reviewer 1's comments:

This paper aims to address a critical gap in atmospheric aerosol modeling by investigating how electrostatic forces influence coagulation processes of dust particles. The authors applied DMA–APS to retrieve joint size-charge distributions of dust aerosols, which can potentially overcome the lack of single-particle charge measurements. By incorporating aerosol charge into the coagulation kernel, their simulations reveal significant electrostatic effects on particle size distribution. Although the topic of paper is interesting, I have doubts on the methodology used in this work, which need to be cleared before a second round of review.

1. The first critical point is the inherent limitations of the DMA–APS setup. The DMA can only select a finite range of particle mobilities, which makes it impossible to select particles with large sizes and only a few charges, as they their mobility is below the selection limit of the DMA. Therefore, the charge measurements are biased towards higher charge state. Such bias challenges the validity of the measurements and must be addressed in the revision.

**Response:** Thank you for this important comment. We think this limitation is indeed there but may not be significant for the dust aerosols in the micrometer size range relevant to this study. The mean charge level for the dust aerosols is on the order of  $10^2 e$ , so these aerosols would generally not fall below the lower DMA mobility selection limit under the present operating conditions. According to the electrical mobility definition equation (Eq. (1)), the lower DMA mobility selection limit used in this study was  $4.68 \times 10^{-9} \text{ m}^2 \cdot \text{V}^{-1} \cdot \text{s}^{-1}$ , which corresponds to a minimum required charge of only  $\sim 5 e$  for an aerosol diameter of  $\sim 1 \mu\text{m}$ ,  $\sim 10 e$  for  $\sim 2 \mu\text{m}$ , and  $\sim 35 e$  even near the upper end of the measured size range ( $\sim 7 \mu\text{m}$ ). Importantly,  $\sim 59\%$  of the total dust aerosol number concentration is distributed within the  $1 - 2 \mu\text{m}$  size range, where the lower DMA mobility boundary corresponds to only  $\sim 5 - 10 e$ . However, the mean charge level of dust aerosols in this dominant  $1 - 2 \mu\text{m}$  size range is still on the order of  $10^2 e$ , much higher than the lower-boundary charge values.

$$n = \frac{3\pi\mu D_p Z_p}{eC} \quad (1)$$

$Z_p$  is the electrical mobility ( $\text{m}^2 \cdot \text{V}^{-1} \cdot \text{s}^{-1}$ ),  $n$  is the number of charges per particle,  $e$  is the elementary charge ( $1.6 \times 10^{-19} \text{ C}$ ),  $\pi$  is the circular constant, and  $\mu$  is the dynamic viscosity of air ( $1.85 \times 10^{-5} \text{ Pa} \cdot \text{s}$  at  $25 \text{ }^\circ\text{C}$ ),  $D_p$  is the electrical mobility diameter (m),  $C$  is the

Cunningham slip correction factor (Seinfeld, J. H., & Pandis, S. N. *Atmospheric Chemistry and Physics: From Air Pollution to Climate Change*. 3rd ed. John Wiley & Sons, 2016).

$C$  is calculated as:

$$C = 1 + \frac{2\lambda}{D} \left[ 1.257 + 0.4 \exp \left( -\frac{1.1D}{2\lambda} \right) \right] \quad (2)$$

$D$  is the aerosol diameter (m),  $\lambda$  is the molecular mean free path ( $68 \times 10^{-9}$  m).

The number fraction of dust aerosols outside the lower DMA mobility limit was estimated on a particle size bin basis. For each particle size bin, the charge value corresponding to the lower DMA mobility boundary was first calculated based on Eq. (1). The number concentration below this boundary was then supplemented based on the fitted charge distribution for that particle size bin. Specifically, the charge distribution in each particle size bin was empirically fitted using a Gaussian-shaped function in  $\ln(n)$  space:

$$N_{D_p}(n) = A_{D_p} \exp \left[ -\frac{(\ln n - \mu_{D_p})^2}{2\sigma_{D_p}^2} \right] \quad (3)$$

where  $n$  is the number of charges per particle,  $D_p$  is the particle diameter of a given size bin,  $N_{D_p}(n)$  is the number concentration at charge state  $n$  for particles with diameter  $D_p$ , and  $A_{D_p}$ ,  $\mu_{D_p}$ , and  $\sigma_{D_p}$  are empirical fitting parameters obtained separately for each particle size bin.

Therefore, under the present DMA operating conditions, only ~0.6% of the dust aerosols in this study are estimated to fall below the lower DMA mobility limit.

In addition, even if the undetected dust aerosol fractions were large, it is also unlikely to substantially affect the results of this study. The contribution of these large weakly charged aerosols to electrostatic coagulation enhancement is expected to be limited. Our measurements show that dust aerosols can exhibit charge distributions significantly higher than those predicted by the Boltzmann charge equilibrium distribution. Such bipolar high-charge characteristics imply a faster electrostatic coagulation rate among dust aerosols (Adachi *et al.*, *Electrostatic coagulation of bipolarly charged aerosol particles*, *Journal of Chemical Engineering of Japan*, 14, 467 – 473, <https://doi.org/10.1252/JCEJ.14.467>, 1981). In contrast, large weakly charged aerosols, with charge levels close to or even lower than those expected under Boltzmann charge equilibrium, are expected to exhibit a much weaker electrostatic coagulation effect.

Furthermore, aerosols with zero charge are explicitly included in the size-charge distribution in this study. Therefore, the potential bias caused by incomplete coverage of low-charge aerosols is not further amplified in the modeling.

#### Changes to the manuscript:

Lines 157-178: In addition, the finite DMA mobility selection range may introduce a small

bias toward higher inferred charge states for large aerosols. This is because aerosols with large diameters and only a few charges may fall below the lower DMA mobility selection limit and therefore cannot be fully selected. According to the electrical mobility definition equation, the lower DMA mobility selection limit used in this study,  $4.68 \times 10^{-9} \text{ m}^2 \cdot \text{V}^{-1} \cdot \text{s}^{-1}$ , corresponds to a minimum required charge of only  $\sim 5$  e for aerosols with diameters of  $\sim 1 \text{ }\mu\text{m}$ ,  $\sim 10$  e for  $\sim 2 \text{ }\mu\text{m}$ , and  $\sim 35$  e even near the upper end of the measured size range ( $\sim 7 \text{ }\mu\text{m}$ ). Importantly,  $\sim 59\%$  of the total dust aerosol number concentration is distributed within the  $1 - 2 \text{ }\mu\text{m}$  size range, where the lower DMA mobility boundary corresponds to only  $\sim 5 - 10$  e. However, the mean charge level of dust aerosols in this dominant  $1 - 2 \text{ }\mu\text{m}$  size range is still on the order of  $10^2$  e, much higher than the lower-boundary charge values.

The number fraction of dust aerosols outside the lower DMA mobility limit was estimated on a particle size bin basis. For each particle size bin, the charge value corresponding to the lower DMA mobility boundary was first calculated based on the electrical mobility definition equation. The number concentration below this boundary was then estimated from the fitted charge distribution for that particle size bin. Specifically, the charge distribution in each particle size bin was empirically fitted using a Gaussian-shaped function in  $\ln(n)$  space:

$$N_{D_p}(n) = A_{D_p} \exp\left[-\frac{(\ln n - \mu_{D_p})^2}{2\sigma_{D_p}^2}\right]$$

where  $n$  is the number of charges per particle,  $D_p$  is the particle diameter of a given size bin,  $N_{D_p}(n)$  is the number concentration at charge state  $n$  for particles with diameter  $D_p$ , and  $A_{D_p}$ ,  $\mu_{D_p}$ , and  $\sigma_{D_p}$  are empirical fitting parameters obtained separately for each particle size bin. Based on this particle size bin based estimation, only  $\sim 0.6\%$  of the dust aerosols in this study are estimated to fall below the lower DMA mobility limit. Therefore, under the present operating conditions, the dust aerosols considered in this study would generally remain above the lower DMA mobility selection limit.

2. For quantitative assessment of the previous point, please add particle size to Table S2 assuming the particle only carries 1 charge. Also, please add the information of DMA sheath flow rate.

**Response:** Thank you for this constructive suggestion. We have added to Table S2 the aerosol diameters corresponding to the prescribed electrical mobility under the assumption of a single elementary charge (1e). In addition, we have added the DMA sheath flow rate used for number of charges per particle measurements of dust aerosols, which was 10 LPM.

**Changes to the manuscript:**

Lines 114-117: The laboratory-generated dust aerosols were then directed into the Differential Mobility Analyzer (DMA, Models 3080 and 3082, TSI Inc., inlet flow rate: 1 LPM, sheath flow rate: 10 LPM) at prescribed electrical mobilities  $Z_p$  (Table S2), and the aerodynamic diameter of the classified aerosols was measured with an APS.

**Changes to the supplement:**

**Lines 117-119:**

**Table S2.** DMA operating electrical mobility  $Z_p$  set points for selecting dust aerosols with specific electrical mobilities.

No.	$Z_p$ ( $\text{m}^2 \cdot \text{V}^{-1} \cdot \text{s}^{-1}$ )	Correspondent aerosol diameter at $Z_p$ for a single charge (1e) ( $\mu\text{m}$ )	Charge number below which 5% of particles fall	Correspondent diameter at 5% charge ( $\mu\text{m}$ )	Median charge number	Correspondent diameter at median charge ( $\mu\text{m}$ )	Charge number below which 95% of particles fall	Correspondent diameter at 95% charge ( $\mu\text{m}$ )
1	$4.68 \times 10^{-9}$	0.197	4	0.784	9	1.765	32	6.275
2	$7.83 \times 10^{-9}$	0.118	5	0.586	16	1.875	56	6.563
3	$1.36 \times 10^{-8}$	0.068	11	0.742	26	1.754	101	6.815
4	$2.48 \times 10^{-8}$	0.037	19	0.703	50	1.85	178	6.586
5	$4.64 \times 10^{-8}$	0.02	37	0.732	91	1.8	334	6.605
6	$8.95 \times 10^{-8}$	0.01	70	0.718	186	1.907	657	6.736
7	$1.76 \times 10^{-7}$	0.005	135	0.704	340	1.773	874	4.557
8	$3.51 \times 10^{-7}$	0.003	299	0.782	567	1.482	932	2.437
9	$7.03 \times 10^{-7}$	0.001	563	0.735	725	0.946	957	1.249

3. The second critical point is that dust particles produced by the dust aerosol generators are representative only of the freshly produced dust particles. After some time in the atmospheres, I would expect their charge state are significantly reduced (as shown in the simulations). Please make this point very clear in the manuscript.

**Response:** Thank you for this important comment. We agree with the reviewer that the aerosols generated by the dust aerosol generator are representative of newly generated or near-source dust aerosols. To avoid over-extrapolation, we have added corresponding clarifications in the revised manuscript.

**Changes to the manuscript:**

Lines 102-103: It should be noted that these aerosols are more representative of freshly generated dust aerosols under near-source conditions than of aged atmospheric dust after

long-range transport.

Lines 334 – 342: The dust aerosols used in this study are more representative of freshly generated dust aerosols. As coagulation and related processes proceed during atmospheric transport, the charge states of dust aerosols are generally expected to decrease. Therefore, the PSD evolution trend shown here is more representative of dust source regions and near-source conditions. However, in real atmospheric transport, dust plumes may continuously mix with newly emitted or entrained aerosols that retain relatively high initial charges. Such continuous input could delay charge decay and sustain stronger electrostatic coagulation over a longer timescale, thereby affecting the timescale of PSD evolution. The above discussion suggests that the transition from freshly generated, highly charged dust to more aged and weakly charged dust during atmospheric transport deserves more explicit consideration in future modeling studies.

4. Is mass conservation checked for the simulation model? It seems that the product particle is put into a single bin rather than distributed between neighboring bins, which is common practice in aerosol simulations with the sectional method (the distribution method is well documented in the literature).

**Response:** Thank you for this valuable comment. We checked the mass conservation. The mechanism of mass loss in the current model is as follows. The mass loss mainly arises from the numerical discretization error introduced when continuously calculated coagulation products are mapped to a single discrete size bin in the current sectional coagulation model. Specifically, when the equivalent volume diameter of a coagulation product does not yet exceed the boundary of the next size interval, the product cannot be partially allocated to the larger bin according to its continuous position. This introduces errors in mass and volume. Even with finer size discretization, this error caused by mapping from a continuous to a discrete representation remains difficult to eliminate completely. It becomes more pronounced in coagulation cases with large aerosol-size differences, such as coagulation between dust aerosols and ambient sub-500 nm aerosols. For example, when a 1.085  $\mu\text{m}$  dust aerosol coagulates with a 21.7 nm ambient sub-500 nm aerosol, the equivalent-volume diameter of the product is

$$D_{new}=(1.085^3+0.0217^3)^{1/3}\approx 1.085003\ \mu\text{m}$$

Since the next larger size bin in the present bin setting is 1.166  $\mu\text{m}$ , this new diameter is still too small to enter the next bin. Therefore, the coagulation product remains assigned to the original 1.085  $\mu\text{m}$  bin in the current sectional model. Accordingly, this error mainly affects the quantitative characterization of the rightward shift of the dust aerosol PSD after coagulation. For clarity, Figure R1 illustrates the mass loss during coagulation induced by size bin discretization.

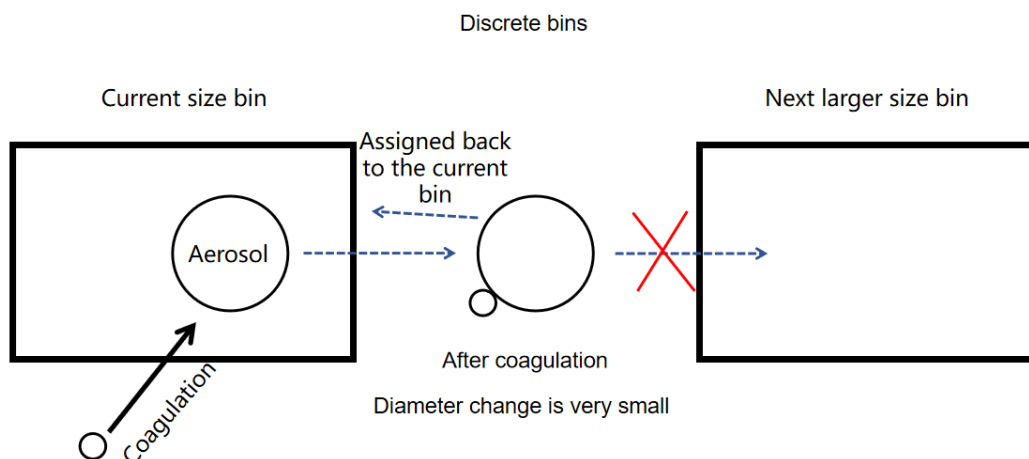


**Figure R1.** Schematic illustration of a coagulation product remaining in the current size bin.

On this basis, we note that the above mass loss has only a limited influence on the differences in PSD evolution between the two coagulation mechanisms. Specifically, this mass loss mainly occurs during the rightward shift of the dust aerosol PSD after coagulation. Assuming constant aerosol density and using the cubic relationship between mass and aerosol diameter, the above  $\sim 10 - 20\%$  mass difference corresponds to an underestimation of the rightward shift of the dust aerosol PSD by  $\sim 3\% - 7\%$ . This is clearly smaller than the magnitude of the differences in PSD evolution caused by the two coagulation mechanisms in this study.

#### Changes to the manuscript:

Lines 383 - 398: It should be noted that, in the mixed aerosol system, the numerical mass loss is more pronounced for coagulation between dust aerosols and ambient sub-500 nm aerosols because of their large size difference. This mass loss mainly arises from the representation of a physically continuous increase in aerosol volume, and thus equivalent diameter, using discrete size bins in the sectional coagulation model. When a dust aerosol coagulates with a much smaller ambient sub-500 nm aerosol, the equivalent-volume diameter of the coagulation product may increase only slightly and may still remain within the original dust aerosol size bin rather than entering the next larger bin. For example, when a  $1.085 \mu\text{m}$  dust aerosol coagulates with a  $21.7 \text{ nm}$  ambient sub-500 nm aerosol, the equivalent-volume diameter of the coagulation product is only approximately  $1.085003 \mu\text{m}$ , which is still below the next larger size bin of  $1.166 \mu\text{m}$ . Therefore, the coagulation product remains assigned to the original  $1.085 \mu\text{m}$  dust aerosol size bin, and the small increase in aerosol volume is not fully reflected as a rightward shift of the dust aerosol PSD. Assuming constant aerosol density and the cubic relationship between aerosol mass and aerosol diameter, a  $\sim 10 - 20\%$  mass loss corresponds to only a  $\sim 3\% - 7\%$  equivalent-diameter difference because aerosol mass scales with the cube of aerosol diameter. Thus, this numerical uncertainty mainly affects the quantitative magnitude of the dust aerosol PSD shift, but is unlikely to alter the qualitative differences in PSD evolution between Brownian coagulation and electrostatic coagulation in the mixed aerosol system.

5. Please elaborate on the method to compile figure 3 from DMA-APS measurements. My understanding is that each DMA-APS measurement at a fixed DMA voltage provide an oblique

line in the mobility diameter-charge space, how are the raw data inverted to give  $dN/d\log dp$ ?

**Response:** The reviewer's understanding is correct that each DMA-APS measurement at a fixed DMA voltage (i.e., under a prescribed electrical mobility condition) corresponds to one oblique line in the size-charge space, as determined according to Eq. (1). The number of charges per particle  $n$  in Eq. (1) was determined from the prescribed electrical mobility  $Z_p$  and the aerodynamic diameter  $D_a$ , which was then converted to the electrical mobility diameter  $D_p$  using Eq. (2). Under each prescribed electrical mobility condition, the APS provided the  $dN/d\log D_p$  values for the DMA-classified dust aerosols over a series of logarithmically spaced particle-diameter bins, i.e., bins with equal intervals in  $\log D_p$ . For each logarithmic particle-diameter bin under each prescribed electrical mobility condition, the corresponding number of charges per particle  $n$  was then calculated from Eq. (1) using the prescribed electrical mobility  $Z_p$  and the converted electrical mobility diameter  $D_p$ . For simplicity, no joint concentration normalization was applied over the particle-size and charge dimensions. The concentration was expressed as  $dN/d\log D_p$ , not as a combined two-dimensional form such as  $dN/(d\log D_p dn)$  or  $dN/(d\log D_p d\log n)$ . Each  $dN/d\log D_p$  value was assigned to the corresponding calculated charge number  $n$ . The size - charge distribution was reconstructed from multiple DMA-APS measurement lines obtained under different prescribed electrical mobility conditions. The bins not directly covered by these measured lines were then filled by linear interpolation of aerosol number concentration between adjacent lines to reconstruct the full two-dimensional distribution.

$$n = \frac{3\pi\mu D_p Z_p}{eC} \quad (1)$$

$Z_p$  is the electrical mobility ( $\text{m}^2 \cdot \text{V}^{-1} \cdot \text{s}^{-1}$ ),  $n$  is the number of charges per particle,  $e$  is the elementary charge ( $1.6 \times 10^{-19}$  C),  $\pi$  is the circular constant, and  $\mu$  is the dynamic viscosity of air ( $1.85 \times 10^{-5}$  Pa·s at 25 °C),  $D_p$  is the electrical mobility diameter (m),  $C$  is the Cunningham slip correction factor (*Seinfeld, J. H., & Pandis, S. N. Atmospheric Chemistry and Physics: From Air Pollution to Climate Change. 3rd ed. John Wiley & Sons, 2016*).

$$D_p = D_a \sqrt{\chi^3 \frac{\rho_0 C(D_m)^2 C(D_a)}{\rho_p C(D_{ve})^3}} \quad (2)$$

is derived from the following two equations:

$$\frac{D_p}{C(D_p)} = \frac{D_{ve}\chi}{C(D_{ve})} \quad (3)$$

$$D_a = D_{ve} \sqrt{\frac{\rho_p C(D_{ve})}{\chi \rho_0 C(D_a)}} \quad (4)$$

$\chi$  is the dynamic shape factor under the experimental conditions (set to 1.0 assuming spherical dust aerosols),  $D_a$  is the aerodynamic diameter (m),  $D_{ve}$  is the volume equivalent diameter (m),  $\rho_0$  is the reference density (1 g/cm<sup>3</sup>), and  $\rho_p$  is the density of dust aerosol particles, taken as 2.65 g/cm<sup>3</sup>.

**Changes to the manuscript:**

Lines 132 - 144: Under each prescribed electrical mobility condition  $Z_p$ , the APS provided the PSD ( $dN/d\log D_p$ ) of the DMA-classified dust aerosols for different aerodynamic diameter bins. The aerodynamic diameter  $D_a$  measured by the APS was converted to the electrical mobility diameter  $D_p$  using Eq. (3). For each logarithmic particle-diameter bin ( $\log D_p$  bin), the corresponding number of charges per particle  $n$  was then calculated from Eq. (1) using the prescribed  $Z_p$  and the converted  $D_p$ . Therefore, each prescribed electrical mobility condition produced one aerosol number concentration line in the two-dimensional size-charge space.

For simplicity, the concentration was not jointly normalized over the particle-size and charge dimensions. It was expressed as  $dN/d\log D_p$ , rather than as a combined two-dimensional concentration form such as  $dN/(d\log D_p dn)$  or  $dN/(d\log D_p d\log n)$ . Each  $dN/d\log D_p$  value was assigned to the corresponding calculated charge number  $n$ . The full two-dimensional size-charge distribution was reconstructed from multiple measured lines obtained under different prescribed electrical mobility conditions, and the bins not directly covered by these measured lines were filled by linear interpolation between adjacent lines.

## Response to Reviewer 2's comments:

This manuscript highlights the important role of electrostatic interactions in aerosol coagulation and their impact on the resulting PSD evolution. The study uses DMA–APS measurements to obtain joint size–charge distributions of aerosols, enabling characterization of single-particle charge properties. Based on this information, the authors combine coagulation modeling with numerical simulations, demonstrating a significant role of highly charged aerosols in the coagulation process. These results help improve understanding of atmospheric aerosol microphysical processes. Overall, the experimental design and modeling framework are generally reasonable; however, several key methodological aspects—such as size conversion, charge data processing, and model parameter assumptions—require further clarification to improve the transparency and reproducibility of the study. In addition, the applicability of some results should be more clearly defined.

1. The manuscript assumes a dynamic shape factor of  $\chi=1$  in the conversion from aerodynamic diameter to electrical mobility diameter. Since mineral dust aerosols are typically irregular in shape, this assumption may introduce a systematic shift in the mapped diameter and therefore alter aerosol bin assignment in the joint size–charge distribution. Given that the reported electrostatic enhancement depends on this joint distribution, please clarify how adopting representative  $\chi$  values for mineral dust ( $\chi>1$ ) would shift the size range associated with highly charged aerosols, and whether such shifts could affect the qualitative conclusions regarding PSD evolution. Clarifying this point would help readers assess the sensitivity of the results to aerosol morphology assumptions.

**Response:** Thank you for raising this important point. We agree that assuming  $\chi = 1$  in the conversion from aerodynamic diameter to electrical mobility diameter may affect the converted electrical mobility diameter range of highly charged dust aerosols. However, this uncertainty does not affect the qualitative comparison between the Brownian-only coagulation and electrostatic coagulation cases, because both cases start from the same initial size – charge distribution and therefore share the same underlying Brownian coagulation pathway, with the only difference being whether electrostatic interactions are included. Therefore, this assumption does not alter the qualitative conclusion of this study that electrostatic interactions substantially enhance coagulation and PSD evolution relative to the Brownian-only case.

### Changes to the manuscript:

Lines 150 – 156: It should also be noted that a dynamic shape factor of  $\chi = 1$  was assumed in the conversion from aerodynamic diameter to electrical mobility diameter as a simplifying assumption. Since irregular mineral dust aerosols typically have  $\chi > 1$ , this assumption may shift the particle size range associated with highly charged aerosols, while this assumption affects the converted particle size, but does not change the measured charge characteristics. This uncertainty does not affect the qualitative comparison between the two cases, because both cases start from the same initial PSD and therefore share the same underlying Brownian coagulation pathway, with the only difference being whether electrostatic interactions are

included.

2. The manuscript uses linear interpolation along the charge axis to fill missing charge-bin concentrations. Since the high-charge tail is inherently sparsely populated, this region is typically sensitive to data-processing methods. When linear interpolation is applied, high-charge bins that would otherwise be zero or undetectable may be assigned non-zero concentrations, thereby artificially smoothing and elevating the tail of the distribution. Given that the reported electrostatic enhancement depends on the fraction and distribution of highly charged aerosols, this treatment may affect the fraction of highly charged aerosols and consequently influence the related analysis results. The authors are therefore encouraged to clarify the robustness of this interpolation step for subsequent analysis results.

**Response:** Thank you for raising this issue. We agree that the high-charge tail, due to its low aerosol number concentrations, can indeed be more sensitive to data-processing methods.

In this study, linear interpolation along the charge axis was applied only to a small number of missing charge bins in the size–charge joint distribution matrix. This was done mainly to preserve the continuity of the matrix for subsequent coagulation modeling. It should be noted that the prescribed  $Z_p$  range in this study is relatively broad, so the covered charge range is also broad and includes the high-charge tail. The high-charge region is therefore not entirely missing, but contains only a small number of discrete gaps. Accordingly, linear interpolation is not expected to significantly increase the proportion of highly charged aerosols.

**Changes to the manuscript:**

Lines 145 – 149: The interpolation uncertainty is mainly associated with the high-charge tail, where aerosol number concentrations are inherently low and therefore more sensitive to data-processing methods. However, the prescribed electrical mobility range in this study is relatively broad and still includes measured points in the high-charge tail. Therefore, the uncertainty associated with the high-charge tail is expected to have a limited influence on the reconstructed size – charge distribution.

3. In the mixed-system simulations, the inclusion of electrostatic interactions leads to an approximately 10% difference in the peak ambient sub-500 nm aerosol number concentration compared with simulations without electrostatic effects. The authors are encouraged to clarify in the Results and Discussion section of the manuscript the significance of this difference for the evaluation of environmental impacts such as radiative forcing and CCN number concentration, and whether it should be highlighted in the discussion of the results or regarded as only a secondary effect within the model. Providing such clarification would help readers better understand the implications of this difference for atmospheric applications.

**Response:** Thank you for raising this issue. We agree that, within the simulation framework of this study, the ~10% difference in the peak number concentration of ambient sub-500 nm aerosols in the mixed system should be regarded as a secondary effect. Nevertheless, it still has environmental relevance because ambient sub-500 nm aerosols contribute substantially to

CCN number concentrations and aerosol radiative effects.

**Changes to the manuscript:**

Lines 359 – 364: Although the magnitude of this difference is modest compared with the much larger the PSD changes of highly charged dust aerosols, the ~10% difference indicates that electrostatic interactions affect the evolution of ambient sub-500 nm aerosols. This effect is environmentally relevant because these aerosols are closely related to aerosol radiative effects and CCN number concentrations. At the same time, it should still be regarded as a secondary effect, as it is much smaller than the PSD changes observed for highly charged dust aerosols themselves.

4. The study adopts a closed-box framework, in which no new aerosol input is considered. Under this assumption, aerosol charges gradually neutralize and decay through coagulation. However, during real atmospheric transport, dust plumes may continuously introduce newly emitted or mixed-in aerosols that can retain relatively high initial charge. Given that the reported electrostatic enhancement depends on the presence of highly charged aerosols, the authors are encouraged to clarify whether such continuous input of highly charged aerosols could delay charge decay and sustain stronger electrostatic coagulation, thereby affecting the reported PSD evolution.

**Response:** Thank you for this important comment. We agree that during real atmospheric transport, if a dust plume continuously mixes with newly emitted or entrained highly charged dust aerosols, this sustained input may indeed slow the charge decay of the system to some extent. It may also allow strong electrostatic coagulation to persist for a longer time, thereby affecting the PSD evolution. In contrast, this study adopts a closed-box framework and does not include any replenishment by newly emitted or entrained highly charged dust aerosols. As a result, the charge level of the system decreases more rapidly than in real atmospheric conditions with continuous input, and the persistence of electrostatic coagulation may therefore be underestimated. Newly emitted or entrained dust aerosols may retain higher charge levels than dust aerosols after long-range transport. However, this does not alter the main conclusion of this study that electrostatic interactions associated with highly charged dust aerosols substantially enhance coagulation relative to the Brownian-only case and thereby accelerate PSD evolution.

**Changes to the manuscript:**

Lines 334 – 342: The dust aerosols used in this study are more representative of freshly generated dust aerosols. As coagulation and related processes proceed during atmospheric transport, the charge states of dust aerosols are generally expected to decrease. Therefore, the PSD evolution trend shown here is more representative of dust source regions and near-source conditions. However, in real atmospheric transport, dust plumes may continuously mix with newly emitted or entrained aerosols that retain relatively high initial charges. Such continuous input could delay charge decay and sustain stronger electrostatic coagulation over a longer timescale, thereby affecting PSD evolution during transport. The above discussion suggests that the transition from freshly generated, highly charged dust to more aged and weakly charged dust during atmospheric transport deserves more explicit

consideration in future modeling studies.

5. In Fig. 3, the caption refers to aerodynamic diameter, whereas the main text indicates that aerosol sizes were converted to mobility diameter. To avoid potential confusion, the authors are encouraged to clarify in the caption which diameter is shown on the x-axis and to ensure consistent terminology between the text and the figure.

**Response:** Thank you for pointing out this issue. The aerosol diameter shown on the x-axis in Fig. 3 is actually the electrical mobility diameter. The original caption incorrectly referred to it as “aerodynamic diameter,” which may have caused confusion. Following the reviewer’s suggestion, we have corrected the caption of Fig. 3 in the revised manuscript and ensured consistent terminology between the main text and the figure caption.